Inorganic Chemistry

Communication

pubs.acs.org/IC

Factors Impacting Electron Transfer in Cyano-Bridged $\{Fe_2Co_2\}$ Clusters

Chunyang Zheng,[†] Juping Xu,[†] Zhixin Yang,[†] Jun Tao,[‡] and Dongfeng Li*[,†,‡]

[†]College of Chemistry, Key Laboratory of Pesticide and Chemical Biology of Ministry of Education, Central China Normal University, 430079 Wuhan, P. R. China

[‡]State Key Laboratory of Physical Chemistry of Solid Surfaces, Xiamen University, Xiamen 361005, P. R. China

Supporting Information

ABSTRACT: A cyano-bridged $\{Fe^{III}{}_2Co^{II}{}_2\}$ complex exhibits reversible thermally and photoinduced intramolecular charge transfer. Its desolvated, MeOH-d_4, and other analogues were compared to disclose the impact factors on the electron-transfer behavior of these $\{Fe^{III}{}_2Co^{II}{}_2\}$ clusters.

Diamagnetic cyano-bridged $\{Fe^{II}{}_{LS}-CN-Co^{III}{}_{LS}\}$ linkages can be excited reversibly by light into paramagnetic $\{Fe^{III}{}_{LS}-CN-Co^{II}{}_{HS}\}$ linkages in a three-dimensional cobalt/iron Prussian blue analogue.[1] This discovery inspired a research area of cyanide-bridged bimetallic complexes, including multidimensional coordination polymers[2,3] and clusters,[2,4−9] which show external stimuli-induced intramolecular electron-transfer behavior with the change of spin states and colors. These bistable molecules with tunable spin states induced by external stimuli are promising candidates for applications in information storage, molecule switches, display devices, etc.[2] Since the Dunbar group first reported the pentanuclear cyano-bridged trigonal-bipyramidal $\{Fe_2Co_3\}$ complex, which exhibits a charge-transfer-induced spin transition (CTIST),[4] many efforts have been devoted to designing and synthesizing such molecule-based materials with CTIST behavior in recent years.[4−9] One of the research goals is to uncover the structure−property relationships of these complexes. A few works have been documented recently to reveal some of the rules and impact factors of the electron-transfer behavior in these mixed-valent clusters.[5,6] However, like spin-crossover compounds, there are many variants (such as ancillary ligands, solvents, anions, hydrogen bonds, $\pi-\pi$ interactions, etc.) capable of influencing the transition of these complexes by means of turn-on/off, tuning of the transition temperature and hysteresis, photoresponse, etc. On the basis of the limited examples, it is still a challenge for chemists to design and control the properties of the complexes with CTIST behavior.

We reported here a new cyano-bridged $\{Fe^{III}{}_2Co^{II}{}_2\}$ square-like complex, $\{[(^{Me}Tp)Fe(CN)_3]_2[Co(bmbpy)_2]_2\}(PF_6)_2\cdot 2MeOH$ [**1**·2MeOH; ^{Me}Tp = methyltris(pyrazolyl)borate, bmbpy = 4,4′-bis(methoxycarbonyl)-2,2′-bipyridine, and MeOH = methanol], which shows intramolecular CTIST behavior triggered by heat and light. In addition, it can transform reversibly to its desolvated form, **1**, in a single crystal-to-single crystal (SC−SC) transition, which exhibits thermally induced intramolecular CTIST at a lower temperature. Furthermore, treatment of the crystals of **1** with MeOH-d_4 will give crystals of **1**·2CD_3OD, which displays also thermally induced CTIST.

Compound **1**·2MeOH was synthesized by mixing of $Co(OTf)_2\cdot 6H_2O$, bmbpy, $(Bu_4N)[(^{Me}Tp)Fe(CN)_3]$, and NBu_4PF_6 in a CH_3CN/MeOH solution at room temperature (see the Supporting Information, SI). Red block crystals of **1**·2MeOH were collected after 6 days by filtration. Single-crystal X-ray diffraction of **1**·2MeOH was performed at 220(2) and 100(2) K (denoted as **1**·2MeOH$^{220\ K}$ and **1**·2MeOH$^{100\ K}$), respectively. The structure of the cation is shown in Figure 1, and the

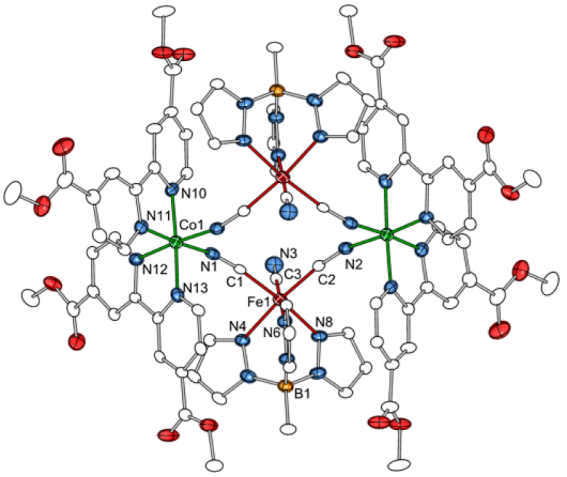

Figure 1. Crystal structure of **1**·2MeOH. The H atoms, solvents, and anions are omitted for clarity.

crystallographic data are listed in Tables S1 and S2 in the SI. Unlike other $\{Fe^{III}{}_2(\mu\text{-}CN)_4Co^{II}{}_2\}$ complexes, such as $\{[(Tp)Fe(CN)_3]_2[Co(4,4'\text{-}bcbpy)_2]_2\}(ClO_4)_2\cdot 2MeOH$ [**2**·2MeOH; Tp = hydrotris(pyrazoleyl)borate, 4,4′-bcbpy = 4,4′-bis(ethoxycarbonyl)-2,2′-bipyridine],[5e] X-ray analysis reveals a seriously distorted square-like $\{Fe_2(\mu\text{-}CN)_4Co_2\}$ structure with an obvious deviation of 180° for all of the Co−N≡C bond angles (**1**·2MeOH$^{100\ K}$: ∠Co1−N1−C1 = 150.1(3), ∠Co1$^{\#1}$−N2−C2 = 152.0(3)°, #1 = 1 − x, 2 − y, 2 − z). These bond angles in **2**·2MeOH are 166.4(2) and 166.6(2)°, respectively.[5e] Also, if we define the four metal centers as a plane, the bridging cyanides reside almost in this plane in **2**·2MeOH, while in **1**·2MeOH, the

Received: October 2, 2015
Published: October 8, 2015

DOI: 10.1021/acs.inorgchem.5b02272
Inorg. Chem. 2015, 54, 9687−9689

cyanides are evidently out of the plane and the $\{Fe_2(\mu\text{-}CN)_4Co_2\}$ core shows a chair conformation like cyclohexane (see Figure S1 in the SI). The average Co−N bond length of the Co1 atom at 100 K is 1.928(3) Å, while the one at 220 K is 2.130(3) Å, implying that the compound is in the high-spin (HS) $\{Fe^{III}_{LS2}Co^{II}_{HS2}\}$ state at 220 K and in the low-spin (LS) $\{Fe^{II}_{LS2}Co^{III}_{LS2}\}$ state at 100 K, respectively.[4−9]

As expected, the terminal cyanides are involved in hydrogen bonding with the lattice MeOH molecules (N3···O1S = 2.920(5) Å at 100 K and 2.940(8) Å at 220 K). Interestingly, the positions of the lattice MeOH molecules change dramatically between the two states. The MeOH molecules show a perpendicular position to the terminal CN groups in the HS structure at 220 K and almost a parallel position to the cyanide in the LS structure at 100 K (see Figure S2 in the SI). We can see that the thermally induced charge-transfer process leads to the mechanical movement of the MeOH molecules, like a reversible heat-driven molecule machine. It can be explained as follows: the shrinking of the bond lengths along the Fe−CN−Co linkages with the transition from the HS to LS state leads to a lesser space for the MeOH molecules, and consequently the surrounding groups push the free MeOH to find another place to accommodate it.

The variable-temperature (VT-)IR spectra were collected in the range of 150−250 K for **1**·2MeOH (see Figure S3 in the SI). The spectrum at 220 K displays three absorptions of cyanide groups, 2143(s), 2135(m), and 2125(w) cm^{-1}, indicating the existence of $\{Fe^{III}-CN-Co^{II}\}$ linkages in the complex.[4−7] The former two peaks can be assigned to the bridging cyanides and the latter one to the terminal cyanides. The split of the peaks for the bridging cyanides confirms the existence of distortion in the structure. With decreasing temperature, the signals for the LS-state $\{Fe^{II}_{LS}-CN-Co^{III}_{LS}\}$ appear with the absorptions at 2095, 2086, 2062, and 2042 cm^{-1}, and the peaks for $Fe^{III}_{LS}-CN-Co^{II}_{HS}$ linkages diminish around 160 K.

The structures at 220 and 100 K and the VT-IR spectra demonstrate the occurrence of electron transfer in **1**·2MeOH. To confirm the transition, the magnetic measurement was performed on the crystalline sample of **1**·2MeOH (Figure 2).

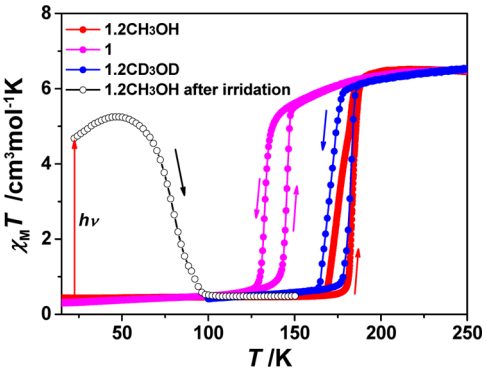

Figure 2. Plots of $\chi_M T$ versus T for **1**·2MeOH, **1**, **1**·2CD_3OD (2000 Oe, 2 K·min^{-1}), and photoexcited **1**·2MeOH (1 T, 2 K·min^{-1}).

The $\chi_M T$ product at 250 K (6.45 cm^3·K·mol^{-1}) agrees with a $\{Fe^{III}_{LS2}Co^{II}_{HS2}\}$ species. With decreasing temperature, the $\chi_M T$ product decreases abruptly at around 180 K to reach a constant value of 0.45 cm^3·K·mol^{-1} below 160 K. The quick drop of the $\chi_M T$ value to a very small residual, evidence of a first-order phase transition, confirms the CTIST behavior in this compound. In the heating mode, the $\chi_M T$ product increases quickly above 175 K to the value of the HS state, demonstrating the reversibly thermally induced CTIST in the molecule. The $T_{1/2}{}^{\downarrow}$ and $T_{1/2}{}^{\uparrow}$ of the reversible process were estimated at ca. 177 and 184 K, respectively.

To study the photoinduced effects, we performed photomagnetic measurements on **1**·2MeOH. The compound is irradiated at 20 K with a laser light (808 nm) under 1 T. The magnetic data increase with the irradiation time, reaching a saturation value after 16 h with $\chi_M T$ = 4.67 cm^3·K·mol^{-1} (see Figure S4 in the SI). The increase of the magnetization suggests the occurrence of a photoinduced charge transfer from $\{Fe^{II}_{LS2}Co^{III}_{LS2}\}$ to a metastable $\{Fe^{III}_{LS2}Co^{II}_{HS2}\}$ phase.[5b,c,g,6a,8a,b] After the irradiation was switched off, the HS state persisted up to about 65 K (see Figure 2).

When exposed to air, **1**·2MeOH lost its lattice MeOH molecules readily to give its desolvated form, **1**, and the crystallinity was well-retained. Single-crystal X-ray diffraction results at 296(2) and 100(2) K (Tables S1 and S2 in the SI) reveal the CTIST behavior in **1**. To determine the transition of **1**, the magnetic measurement was performed on the crystalline powder of **1** (Figure 2). The $\chi_M T$ product at 250 K (6.49 cm^3·K·mol^{-1}) is consistent with the HS state. With decreasing temperature until ca. 150 K, the $\chi_M T$ product decreases slowly to 5.63 cm^3·K·mol^{-1}, which is due to a small portion of the clusters with gradual CTIST (see the VT-IR spectra in Figure S5 in the SI) and the spin−orbit coupling effects of cobalt(II)[11] in the complex. Below ca. 140 K, the value of $\chi_M T$ drops sharply at around 130 K to reach a small residual value of 0.39 cm^3·K·mol^{-1} at 100 K. Upon heating, the $\chi_M T$ value increases swiftly at ca. 149 K to the same value as that before the temperature decreased. $T_{1/2}{}^{\downarrow}$ and $T_{1/2}{}^{\uparrow}$ of the CTIST behavior were estimated at ca. 130 and 142 K, respectively, with 12 K hysteresis. Apparently, the transition temperatures for **1** are much lower than those for **1**·2MeOH. According to the difference in the structures of these compounds, we tentatively conclude that the hydrogen bonding (between the terminal cyanides and the lattice MeOH) in **1**·2MeOH plays the key role in affecting the transition temperature.

Complex **1** can reabsorb MeOH to recover to **1**·2MeOH in a SC−SC transformation manner. To explore the isotropic effect of hydrogen bonding to the transition, we treated **1** in MeOH-d_4 to give **1**·2CD_3OD with good crystallinity (see Tables S1 and S2 in the SI for the crystallographic data). The magnetic data show that $T_{1/2}{}^{\downarrow}$ and $T_{1/2}{}^{\uparrow}$ of the reversible CTIST process were estimated at ca. 171 and 182 K, respectively, showing an 11 K hysteresis. The result demonstrates that the isotropic hydrogen-bonding effect can only fine-tune the transition to a slightly lower temperature, which agrees with the fact that the smaller Z/r ratio of the D atom than the H atom will give a weaker hydrogen-bonding interaction.

Complex **2**·2MeOH,[5e] a close analogue of **1**·2MeOH, keeps the LS state in the measurable temperature range. We found that the green color of the crystals of **2**·2MeOH is retained even in boiling MeOH solvent, meaning that the transition temperature from the LS to HS state for this compound is higher than 337 K, while complex **1**·2MeOH shows a CTIST behavior below ca. 180 K. The notable difference in their properties is considered to be derived from the differences in the structures. First, the methyl group on the B atom in $^{Me}Tp^-$ acting as an electron donor will lead to a lower $Fe^{III/II}$ redox potential and transition temperature for **1**·2MeOH, which was well discussed in a recent paper.[5g] However, only one methyl group, a weak electron donor away from the pyrazole ring, will not pronouncedly affect the transition temperature, which is evidenced by almost the same $Fe^{III/II}$ redox

DOI: 10.1021/acs.inorgchem.5b02272
Inorg. Chem. 2015, 54, 9687−9689

potentials for the tricyanide building blocks ($E_{1/2}$ = −0.79 for Tp vs −0.80 mV for ^{Me}Tp).[5g,10] Second, as mentioned in the X-ray structure, compound **1**·2MeOH has highly bent ∠Co−N≡C angles and a distorted $\{Fe_2(\mu\text{-}CN)_4Co_2\}$ core, which will hinder the effective formation of σ and π bonds of Co−$N_{C\equiv N}$ and markedly impair electron delocalization of the molecule through the Co^{II} centers. As a result, more charge on the bridging cyanides will weaken their π acceptance, enhance Fe → C≡N π-back-donation, lead to C≡N bond weakening and a concomitant lowering of $\nu_{C\equiv N}$, and give lower redox potentials of Fe centers (lower transition temperature). In fact, we did observe the much smaller value of $\nu_{C\equiv N}$ in **1**·2MeOH. For the analogues of complex **1** and the desolvated form of **2**·2MeOH (**2**),[5e] the ∠Co−N≡C angles and the stretching vibration of the bridging cyanides are 150.9(3) and 148.4(3)° and 2143 cm^{-1} for **1** and 174.4(9) and 179.2(12)° and 2168 cm^{-1} for the latter,[5e] respectively. The remarkable red shift of $\nu_{C\equiv N}$ for **1** should be attributed to distortion of the Fe^{III}−CN−Co^{II} linkages. Moreover, different from **1**, complex **2** displays CTIST below 250 K.[5e] The facts indicate that the bent ∠Co−N≡C angles and distortion of the $\{Fe_2(\mu\text{-}CN)_4Co_2\}$ core are the key factors for lowering of the transition temperature in **1**·2MeOH and **1** compared to its analogues.

Hysteresis loops are found in the family of complex **1**·2MeOH, while complex **2** shows a crossover behavior and no hysteresis.[5e] It is believed that the cooperativity of intermolecular elastic interactions can lead to first-order phase transition and hysteresis.[5b] Structure analysis indicates that there are no effective intermolecular π−π-stacking interactions between the bipyridine rings in the structures of **1**·2MeOH, **1**, and **1**·2CD_3OD. However, rather strong nonclassical hydrogen bonds (C−H···O) were found in these compounds between the carbonyl O atoms (O1 and O7) and the adjacent C atoms (C28 and C23) of bipyridine groups (**1**·2MeOH$^{100\ K}$: O1···C28$^{\#2}$ = 2.884(4) Å, #2 = 1 − x, 1 − y, 2 − z; O7···C23$^{\#3}$ = 2.949(4) Å, #3 = −x, 2 − y, 2 − z; see Table S2 and Figure S6 in the SI). For complex **2**,[5e] the bigger ethyl groups separating the squares eliminate the intermolecular π−π interactions and the nonclassical hydrogen bonds, thus leading to the crossover behavior and no hysteresis.

■ ASSOCIATED CONTENT

Supporting Information

The Supporting Information is available free of charge on the ACS Publications website at DOI: 10.1021/acs.inorgchem.5b02272.

Synthetic, spectroscopic, crystallographic, and magnetic data (PDF)

X-ray crystallorgraphic data in CIF format (CIF)

■ AUTHOR INFORMATION

Corresponding Author

*E-mail: dfli@mail.ccnu.edu.cn.

Notes

The authors declare no competing financial interest.

■ ACKNOWLEDGMENTS

We thankful for support from the NNSF of China (Grants 21471063 and 21172084) and self-determined research funds of CCNU from the colleges' basic research and operation of MOE.

■ REFERENCES

(1) Sato, O.; Iyoda, T.; Fujishima, A.; Hashimoto, K. *Science* **1996**, *272*, 704−705.

(2) (a) Halcrow, M. A.; Dunbar, K. R.; Achim, C.; Shatruk, M. *Charge Transfer-Induced Spin-Transitions in Cyanometalate Materials*; Wiley: New York, 2013. (b) Sato, O.; Tao, J.; Zhang, Y.-Z. *Angew. Chem., Int. Ed.* **2007**, *46*, 2152−2187.

(3) For example: (a) Bleuzen, A.; Lomenech, C.; Escax, V.; Villain, F.; Varret, F.; Cartierdit Moulin, C.; Verdaguer, M. *J. Am. Chem. Soc.* **2000**, *122*, 6648−6652. (b) Arimoto, Y.; Ohkoshi, S.; Zhong, Z. J.; Seino, H.; Mizobe, Y.; Hashimoto, K. *J. Am. Chem. Soc.* **2003**, *125*, 9240−9241. (c) Cafun, J. D.; Champion, G.; Arrio, M. A.; dit Moulin, C. C.; Bleuzen, A. *J. Am. Chem. Soc.* **2010**, *132*, 11552−11559.

(4) (a) Berlinguette, C. P.; Dragulescu-Andrasi, A.; Sieber, A.; Galán-Mascarós, J. R.; Güdel, H.-U.; Achim, C.; Dunbar, K. R. *J. Am. Chem. Soc.* **2004**, *126*, 6222−6223. (b) Berlinguette, C. P.; Dragulescu-Andrasi, A.; Sieber, A.; Güdel, H.-U.; Achim, C.; Dunbar, K. R. *J. Am. Chem. Soc.* **2005**, *127*, 6766−6779. (c) Hilfiger, M. G.; Chen, M.; Brinzari, T. V.; Nocera, T. M.; Shatruk, M.; Petasis, D. T.; Musfeldt, J. L.; Achim, C.; Dunbar, K. R. *Angew. Chem., Int. Ed.* **2010**, *49*, 1410−1413. (d) Avendano, C.; Hilfiger, M. G.; Prosvirin, A.; Sanders, C.; Stepien, D.; Dunbar, K. R. *J. Am. Chem. Soc.* **2010**, *132*, 13123−13125. (e) Funck, K. E.; Prosvirin, A. V.; Mathonière, C.; Clérac, R.; Dunbar, K. R. *Inorg. Chem.* **2011**, *50*, 2782−2789.

(5) (a) Li, D.-F.; Clérac, R.; Roubeau, O.; Harté, E.; Mathonière, C.; Le Bris, R.; Holmes, S. M. *J. Am. Chem. Soc.* **2008**, *130*, 252−258. (b) Zhang, Y. Z.; Li, D.-F.; Clérac, R.; Kalisz, M.; Mathonière, C.; Holmes, S. M. *Angew. Chem., Int. Ed.* **2010**, *49*, 2941−2944. (c) Siretanu, D.; Li, D.-F.; Buisson, L.; Bassani, D. M.; Holmes, S. M.; Mathonière, C.; Clérac, R. *Chem. - Eur. J.* **2011**, *17*, 11704−11708. (d) Jeon, I.-R.; Calancea, S.; Panja, A.; Piñero Cruz, D. M.; Koumousi, E. S.; Dechambenoit, P.; Coulon, C.; Wattiaux, A.; Rosa, P.; Mathonière, C.; Clérac, R. *Chem. Sci.* **2013**, *4*, 2463−2470. (e) Cao, L.; Tao, J.; Gao, Q.; Liu, T.; Xia, Z.; Li, D. *Chem. Commun.* **2014**, *50*, 1665. (f) Koumousi, E. S.; Jeon, I.-R.; Gao, Q.; Dechambenoit, P.; Woodruff, D. N.; Merzeau, P.; Buisson, L.; Jia, X. L.; Li, D.-F.; Volatron, F.; Mathonière, C.; Clérac, R. *J. Am. Chem. Soc.* **2014**, *136*, 15461. (g) Zhang, Y.-Z.; Ferko, P.; Siretanu, D.; Ababei, R.; Rath, N. P.; Shaw, M. J.; Clérac, R.; Mathonière, C.; Holmes, S. M. *J. Am. Chem. Soc.* **2014**, *136*, 16854−16864.

(6) (a) Nihei, M.; Sekine, Y.; Suganami, N.; Nakazawa, K.; Nakao, A.; Nakao, H.; Murakami, Y.; Oshio, H. *J. Am. Chem. Soc.* **2011**, *133*, 3592−3600. (b) Mitsumoto, K.; Oshiro, E.; Nishikawa, H.; Shiga, T.; Yamamura, Y.; Saito, K.; Oshio, H. *Chem. - Eur. J.* **2011**, *17*, 9612−9618. (c) Nihei, M.; Okamoto, Y.; Sekine, Y.; Hoshino, N.; Shiga, T.; Liu, I. P.-C.; Oshio, H. *Angew. Chem., Int. Ed.* **2012**, *51*, 6361−6364. (d) Hoshino, N.; Iijima, F.; Newton, G. N.; Yoshida, N.; Shiga, T.; Nojiri, H.; Nakao, A.; Kumai, R.; Murakami, Y.; Oshio, H. *Nat. Chem.* **2012**, *4*, 921−926. (e) Newton, G. N.; Mitsumoto, K.; Wei, R.; Iijima, F.; Shiga, T.; Nishikawa, H.; Oshio, H. *Angew. Chem., Int. Ed.* **2014**, *53*, 2941−2944.

(7) (a) Liu, T.; Zhang, Y.; Kanegawa, S.; Kang, S.; Sato, O. *Angew. Chem., Int. Ed.* **2010**, *49*, 8645−8648. (b) Liu, T.; Zhang, Y.; Kanegawa, S.; Sato, O. *J. Am. Chem. Soc.* **2010**, *132*, 8250−8251. (c) Liu, T.; Dong, D.-P.; Kanegawa, S.; Kang, S.; Sato, O.; Shiota, Y.; Yoshizawa, K.; Hayami, S.; Wu, S.; He, C.; Duan, C.-Y. *Angew. Chem., Int. Ed.* **2012**, *51*, 4367−4370. (d) Dong, D.-P.; Liu, T.; Kanegawa, S.; Kang, S.; Sato, O.; He, C.; Duan, C.-Y. *Angew. Chem., Int. Ed.* **2012**, *51*, 5119−5123.

(8) (a) Mercurol, J.; Li, Y.; Pardo, E.; Risset, O.; Seuleiman, M.; Rousselière, H.; Lescouëzec, R.; Julve, M. *Chem. Commun.* **2010**, *46*, 8995−8997. (b) Mondal, A.; Li, Y.; Seuleiman, M.; Julve, M.; Toupet, L.; Buron-Le Cointe, M.; Lescouëzec, R. *J. Am. Chem. Soc.* **2013**, *135*, 1653−1656. (c) Mondal, A.; Chamoreau, L.-M.; Li, Y.; Journaux, Y.; Seuleiman, M.; Lescouëzec, R. *Chem. - Eur. J.* **2013**, *19*, 7682−7685.

(9) Podgajny, R.; Chorazy, S.; Nitek, W.; Rams, M.; Majcher, A. M.; Marszałek, B.; Żukrowski, J.; Kapusta, C.; Sieklucka, B. *Angew. Chem., Int. Ed.* **2013**, *52*, 896−900.

(10) Wang, C.-F.; Liu, W.; Song, Y.; Zhou, X.-H.; Zuo, J.-L.; You, X.-Z. *Eur. J. Inorg. Chem.* **2008**, *2008*, 717−727.

(11) Li, D.-F.; Parkin, S.; Wang, G.; Yee, G. T.; Prosvirin, A. V.; Holmes, S. M. *Inorg. Chem.* **2005**, *44*, 4903−4905.

DOI: 10.1021/acs.inorgchem.5b02272
Inorg. Chem. 2015, 54, 9687−9689